The Electrochemical Society
Advancing solid state & electrochemical science & technology

Design of a Single-Ion Conducting Polymer Electrolyte for Sodium-Ion Batteries

View the article online for updates and enhancements.

Design of a Single-Ion Conducting Polymer Electrolyte for Sodium-Ion Batteries

Kewei Liu,[1] Yingying Xie,[1] Zhenzhen Yang,[1] Hong-Keun Kim,[2] Trevor L. Dzwiniel,[3] Jianzhong Yang,[1] Hui Xiong,[4,5] and Chen Liao[1,6,z]

[1]*Chemical Sciences and Engineering Division, Argonne National Laboratory, Lemont, Illinois 60439, United States of America*
[2]*Department of Mechanical Engineering, Inha University, Michuhol-Gu, Incheon 22212, Republic of Korea*
[3]*Applied Materials Division, Argonne National Laboratory, Argonne, Illinois 60439, United States of America*
[4]*Micron School of Materials Science and Engineering, Boise State University, Boise, Idaho 83725, United States of America*
[5]*Center for Advanced Energy Studies, Idaho Falls, Idaho 83401, United States of America*
[6]*Joint Center for Energy Storage Research, Argonne National Lab, Lemont, Illinois 60439, United States of America*

A sodium bis(fluoroallyl)malonato borate salt (NaBFMB) is synthesized. Using a Click thiol-ene reaction, NaBFMB can be photo-crosslinked with a tri-thiol (trimethylolpropane tris(3-mercapto propionate), TMPT) to create a single-ion conducting electrolyte (NaSIE), with all negative charges residing on the borate moieties and anions immobilized through the 3-D crosslinked network. The NaSIE can be prepared either as a free-standing film or through a drop-cast method followed by a photo crosslinking method for an in-situ formation on top of the electrodes. The free-standing film of NaSIE has a high ionic conductivity of 2×10^{-3} S cm^{-1} at 30 °C, and a high transference number (t_{Na}^{+}) of 0.91 as measured through the Bruce-Vincent method. The electrochemical stability of NaSIE polymer electrolyte is demonstrated via cyclic voltammetry (CV) to be stable up to 5 V vs Na/Na^{+}. When tested inside a symmetrical Na//Na cell, the NaSIE shows a critical current density (CCD) of 0.4 mA cm^{-2}. The stability of NaSIE is further demonstrated via a long cycling of the stripping/plating test with a current density of 0.1 mA cm^{-2} at five-minute intervals for over 10,000 min. Using the in-situ method, NaSIE is used as the electrolyte for a sodium metal battery using P2 (Na resides at prismatic sites with ABBAAB stacking)-cathode of Na$_{0.67}$Ni$_{0.33}$Mn$_{0.67}$O$_2$ (NNMO) and is cycled between the cut-off voltages of 2.0–4.0 V. A high initial specific capacity (85.7 mAh g^{-1}) with a capacity retention of 86.79% after 150 cycles is obtained. © 2021 The Electrochemical Society ("ECS"). Published on behalf of ECS by IOP Publishing Limited. [DOI: 10.1149/1945-7111/ac42f2]

One of the biggest challenges facing the humankind is the energy crisis: as the population grows, the traditional way of energy production from burning fossil fuels leads to increased CO_2 emissions and climate change. Renewable energy such as wind, sun, and tides is desired, yet their intermittent nature requires large-scale energy storage systems. Despite the ubiquity of lithium ion batteries (LIBs) applications in consumer electronics, the adoption of LIBs into larger formats such as electric vehicles and grid storage faces more challenges. For example, a big hurdle is the limited supply of lithium, an indispensable element in LIBs, which has a low earth abundance of 0.002–0.006 wt%. On the other hand, sodium in the same alkali metal group, is earth abundant (existing mostly as NaCl in seawater) and has a high electropositivity and a high specific gravimetric energy density (1166 mA h g^{-1}). With physical and chemical properties similar to lithium, sodium would also make the industrial adoption seamless, as it works well with aluminum current collectors without observation of alloy formation.[1]

Several challenges of sodium ion batteries exist: limited choices of high purity electrolytes, the propensity for sodium dendrite formation, and consequent high reactivity of sodium dendrites with electrolytes. To mitigate the hazards associated with sodium metal, approaches of using solid/gel electrolyte are adapted. There have been numerous reports[2–5]; for example, Qi et al. reported the usage of a polymer electrolyte consisting of (sodium bis(trifluoromethanesulfonyl)imide/polyetheylene oxide, NaTFSI/PEO) with cathodes such as the layered transition metal oxide Na$_{0.67}$Ni$_{0.33}$Mn$_{0.67}$O$_2$ (NNMO) and NASICON Na$_3$V$_2$(PO$_4$)$_3$ (NVP).[6] Li et al. reported a 3-D lithium poly tartaric acid borate single-ion conducting electrolyte with a highly reversible specific capacity of 80 mAh g^{-1}.[7]

Here, we report the synthesis and application of a novel sodium single-ion conducting electrolyte consisting of a sodium bis(fluoroallyl)malonato borate salt (NaBFMB). Thiol-ene reaction, a niche Click reaction, is used here because of its high efficiency, the high tolerance of functional groups, and mild conditions. The fast photo-crosslinking of the thiol-ene reaction ensured the close contact of the electrolyte and electrode to obtain a minimal impedance in the cell. In the single-ion conducting electrolyte, all negative charges reside on borate moieties, which are immobilized through the 3-D cross-linked network. The single-ion nature will be reflected by a high transference number indicating unimodal Na^{+} transport for the ions. Traditionally, an electrochemical polarization method or diffusivity measurement can be used to determine the transference number, with the former relying on the assumption that the steady state current is mostly due to Na^{+}, that the initial current is due to both Na^{+} and anions and finally, that the current due to Na^{+} does not change significantly with time. The Bruce-Vincent method modifies the DC polarization measurement by introducing a simple way of using impedance spectra.[8] A close steady-state current to an initial current would indicate a high transference number. Indeed, a high transference number t_{Na}^{+} of 0.91 is obtained. The P2-Na$_{0.67}$Ni$_{0.33}$Mn$_{0.67}$O$_2$ (NNMO) cathode is used to test the performance of the newly developed NaSIE electrolyte as it has a high theoretical capacity of 173 mAh g^{-1}.

Experimental Sections

Synthesis of NaBFMB.—The synthesis of 2-allyl-2-fluoro malonic acid was published previously.[9] A mixture of 2-allyl-2-fluoro malonic acid (10.00 g, 61.68 mmol, 1.00 equivalent), sodium carbonate (1.64g, 15.47 mmol, 0.25 eq), and boric acid (1.91g, 30.87 mmol, 0.50 eq) was added to a 500ml 2-necked round-bottom flask equipped with a thermocouple probe. Then, 250 ml of diethyl carbonate was introduced with continued stirring. The mixture was heated to reflux under reduced pressure for six hours and a Dean-Stark trap filled with 3Å molecular sieves was attached to the flask. The reaction mixture was then cooled under nitrogen and filtered, washed with diethyl carbonate (DEC), and again with 20ml dry MTBE (tert-Butyl methyl ether) before drying in a vacuum oven at 60°C. A white powder was collected. To further purify the NaBFMB

salt, 2.4 g crude material was added to 20 ml hot acetonitrile and the suspension was filtered and concentrated with rotary evaporation. 1.5 g NaBFMB salt was obtained after vacuum drying.

Preparation of free-standing NaSIE and NaSIE coated electrodes.—A mixture of 0.5 mmol NaBFMB, 0.33 mmol trimethylolpropane tris(3-mercapto propionate) (TMPT) and 0.05 mmol 2,2-dimethoxy-2-phenylacetophenone (DMPA) was dissolved in a 0.6 ml mixture of propylene carbonate (PC) and sulfolane (SF) with a volume ratio of 1:2 in an argon-filled glovebox. The liquid precursor was then added to a customized Teflon mold. After 15 min of UV–vis light exposure, the cross-linked NaSIE polymer film was obtained. To prepare the NaSIE-coated electrodes, the liquid precursor was drop-casted onto the sodium metal (7/16 inch) and ($Na_{0.67}Ni_{0.33}Mn_{0.67}O_2$) NNMO electrode disc (10 mm), respectively. A 15-min. rest was required prior to the 15-min. UV curing.

Cathode syntheses.—Pure P2-$Na_{0.67}Ni_{0.33}Mn_{0.67}O_2$ material was prepared by a solid-state reaction using co-precipitated precursor $Ni_{0.33}Mn_{0.67}(OH)_2$ with Na_2CO_3 salts.[10] The $Ni_{0.33}Mn_{0.67}(OH)_2$ precursor was prepared through co-precipitation following a similar method described by Dahn et al.[10,11] Then the $Ni_{0.33}Mn_{0.67}(OH)_2$ powder and Na_2CO_3 were thoroughly mixed stoichiometrically with a ratio of 2:1.1 for a pure P2-$Na_{0.67}Ni_{0.33}Mn_{0.67}O_2$. The mixed powder was then calcined at 850 °C for 20 h in air. The furnace was then switched off and allowed to cool down to 500 °C, at which time the sample was removed from the furnace and air-cooled to room temperature. The final product was then transferred to the glovebox to avoid exposure to moisture in air.

Cell fabrication.—A slurry consisting of 80% wt NNMO, 10% wt C45, and 10% wt PVDF (polyvinylidene fluoride) in NMP (N-methyl-2-pyrrolidone) was prepared and casted on to an aluminum foil with a doctor blade and dried at 80 °C overnight to achieve the NNMO laminates with an active material loading of ~1.6 mg cm^{-2}. The laminates were further heated at 110 °C under vacuum for 12 h to remove the solvent residues. The NaSIE coated sodium and NNMP electrodes were compressed together with a 10 mm gasket and fabricated into 2032-type stainless steel coin cells in an argon-filled glovebox.

Electrochemical characterization.—The electrochemical study was performed on a Solartron Analytical 1400 Cell Test System. A symmetrical stainless steel/NaSIE (1/2 inch)/stainless steel cell is utilized for the ionic conductivity test in temperatures ranging from 20 to 80 °C, where the impedance of the cell is obtained in the frequency range of 1 MHz to 0.1 Hz at the open circuit potential (OCV) at an amplitude of 10 mV. The electrochemical stability test was carried out in the Na/NaSIE/stainless steel (ss) cells with a voltage range between −0.5V to 5V at a scan rate of 0.5 mV s^{-1}. The sodium transference number was measured via a Bruce-Vincent method reported elsewhere.[12]

X-ray photoelectron spectroscopy measurement (XPS).—XPS analysis was carried out in a PHI 5000 VersaProbe II system (Physical Electronics) attached to an Ar-atmosphere glovebox. The samples were transferred into the XPS chamber through the glovebox without ambient air exposure. The high-resolution spectra of each element were collected under the following conditions: pass energy of 23.25 eV, 100 μm beam (25 W) with Al Kα radiation (hυ = 1486.6 eV) and electron beam sample neutralization, fixed analyzer transmission mode. The thickness of SEI layer on the Na anode was evaluated by Ar$^+$ depth profiling. The sputtering process was carried out at 2KeV for 8 min with 1 min interval.

Scanning electron microscopy (SEM).—As described in an earlier work,[13] cycled electrodes were placed in an airtight holder during transferring into SEM chamber without exposure to the air.

SEM images were taken from JEOL JSM-6610LV and EDS was performed with Oxford EDS detector.

^{1}H Nuclear magnetic resonance (NMR) analysis.—The cycled cells were disassembled in an argon-filled glovebox, and the cycled electrolyte was collected by dipping the electrodes and the separators in 1.0 ml CDCl$_3$. The resulting solutions were subjected to ^{1}H NMR analyses. NMR spectra were obtained with a Bruker Avance III HD 300 MHz spectrometer, while the chemical shifts in parts per million (δ, ppm) were referenced to CDCl$_3$ at 7.26 ppm.

Results and Discussions

Synthetic design.—Although it may seem too fundamental to be relevant to electrochemical performance, the chemistry of how the monomer is designed and what synthetic approach was used to construct the surface is actually essential to improve the performance. The monomer, sodium bis(fluoroallyl)malonato borate (NaBFMB), is synthesized for the first time. Note the anions are exclusively residing on the borates, which has been reported to have weak coordination and benign electrochemistry towards lithium ion and lithium metal batteries. Since sodium metal batteries (SMBs) are similar in many ways to lithium metal batteries (LMBs), including their reduction potential, their alloying properties, we can borrow the same synthetic moiety from LMBs to SMBs. In fact, the synthetic route is based on the procedure of making the lithium analog (LiBFSIE), which we reported previously with a few changes.[14] However, the introduction of a new complexing cation of Na$^+$ instead of Li$^+$, despite the weak coordination of the borate centered anion, changes the solubility of the new NaFBMB salt drastically from that of LiBFSIE. The change of solubility would reflect in the choice of the solvents as plasticizers: only solvents with both good solvating power and high electrochemical properties can be used as plasticizers. The purity of the salt is also essential as presence of impurity can lead to parasitic reactions, decrease electrochemical stability, and cause a lower coulombic efficiency. The purity of the NaFBMB is significantly improved through repeated recrystallization with anhydrous CH$_3$CN. Like its Li analog,[14] a non-coordinating sp^3 boron center couples with Na$^+$ and demonstrates a low dissociation energy and a high ionic conductivity. The electrochemical and chemical stability of the anion is also significantly improved by incorporating the fluorine substitution and eliminating the α-H with the allyl groups in $-O-C(=O)-C(F)(allyl)-O-C$ $(=O)-$ malonato moiety. The solubility of NaBFMB is dramatically different from that of the LiBFMB in terms of their preferred solvents and concentration. For example, LiBFMB shows a similar solubility as LiPF$_6$ and lithium bis(oxalate) borate (LiBOB), with a reasonably high concentration in a mixture of carbonates. NaBFMB, on the other hand, only shows appreciable solubility in sulfolane and PC, both of which are solvents with a high dielectric constant ($\varepsilon =$ 43.3 and 64 F m^{-1}, respectively). A mixture of sulfolane and propylene carbonate (PC) is utilized as the plasticizer for its optimized ionic conductivity and sodium ion transport.

The NMR spectra of the purified NaBFMB are shown in Fig. 1. The ^{1}H NMR display a typical allyl group proton splitting pattern ($\delta = 5.7$–5.9 ppm, m, 1H, 5.16–5.3, m, 1H, 2.8–3.0, m, 1H, 1.86–2.0, m, 2H), the ^{19}F NMR displays a triplet pattern, and ^{11}B NMR shows a sharp singlet.

Interface plays a big role in both conventional LIB and solid-state batteries, especially the latter, due to the tendencies of formation of voids, and imperfect contact of two surfaces that results in high impedance and dendrite formation.[15] Using the previous strategy we have in constructing interface, which requires a few elements in formation of the electrolyte/electrode interface: (1) a fluidic precursor to ensure the coverage of the pores inside the cathode electrode. Unlike the electrodes used in catalysis, the battery electrodes are made of a "mess," with tortuosity up to 30%, and materials consisting of binder (PVDF), carbon black (particles),
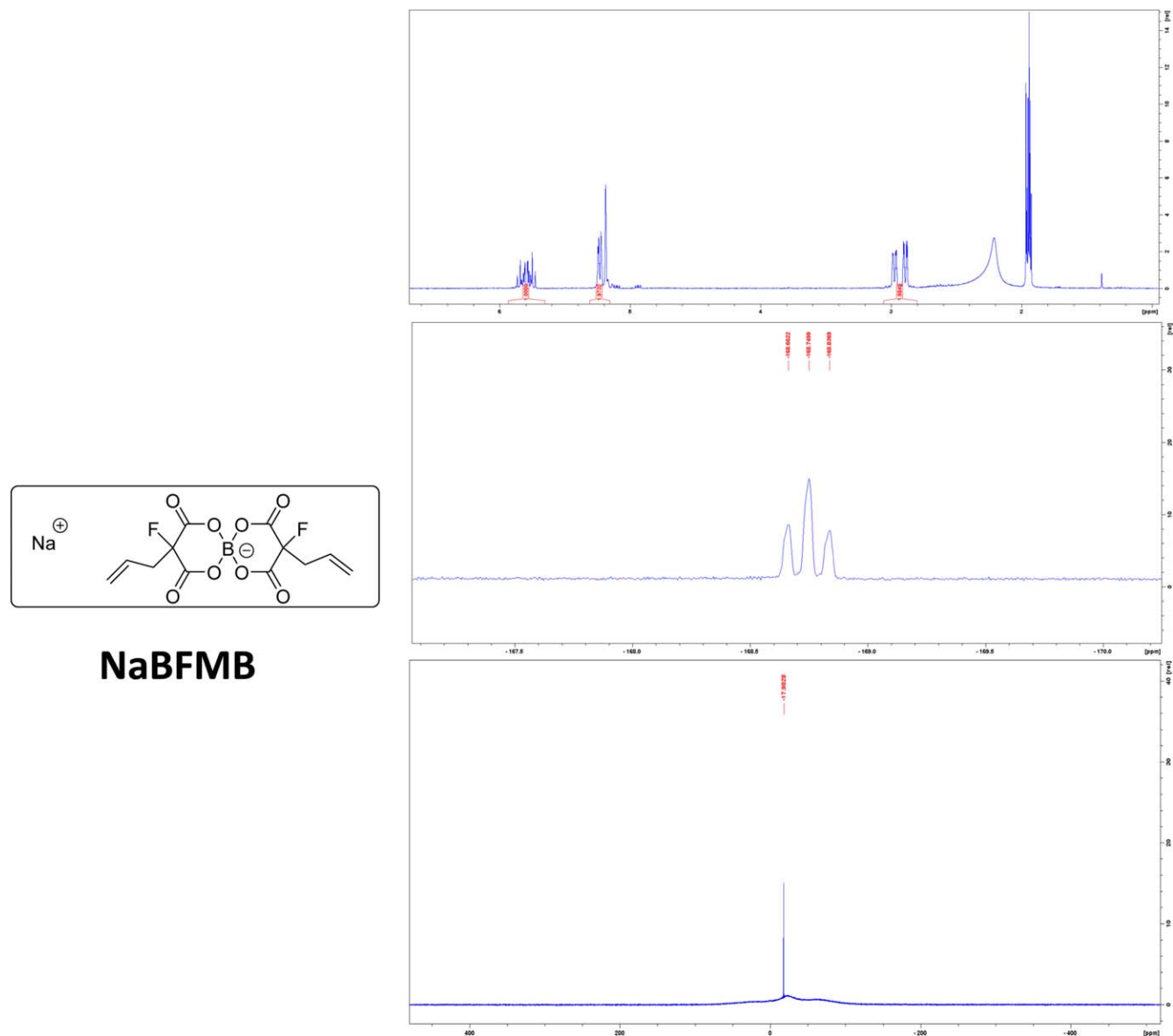
Figure 1. The ^{1}H NMR, ^{19}F NMR, and ^{11}B NMR of the purified NaBFMB. The broad background in ^{11}B NMR was attributed to the use of glass NMR tube (sodium borosilicate).

electrode active materials (NNMO in this case), and porous structure is essential for the performance. If a solid hard electrolyte is used, it is very hard for the electrolyte to penetrate the electrode and form good contact. Without the good contact of the electrode/electrolyte, impedance rise will be exacerbated and not a high utilization of the electrode will be realized. With that in mind, we design a fluidic precursor that can infiltrate into a free-standing film, or in situ film on top of the electrodes within 15 min of photo crosslinking. To ensure a fast curing, the NaSIE polymer electrolyte is conveniently synthesized via a thiol-ene reaction, in which the allyl group reacts with an alkyl thiol via an anti-Markovnikov reaction. The chemical structure of the polymer electrolyte is demonstrated in Fig. 2a: the thiol-ene reaction ensures a highly efficient and high-yield polymerization reaction, hence the almost perfect interface. The NaBFMB salt is designed with two allyl groups for the thiol-ene reactions.

To mitigate the interfacial issues in the batteries equipped with polymer electrolyte, in situ polymerization is carried out on the electrodes. The NaSIE liquid precursor was drop-casted on the NNMO cathode, in which the liquid is able to infiltrate the porous structure inside the heterogeneous porous cathode materials (Fig. 2b).

After a 15-min. UV exposure, the liquid precursor is sufficiently cured to enable the tight contact between the polymer electrolyte and cathode particles, facilitating the sodium transport across the interface. Furthermore, NaSIE was coated onto the sodium metal anode surface. The adhesive nature of the polymeric NaSIE enables good contact when the cell is assembled by compressing the NaSIE-coated sodium and NaSIE-coated cathode laminate.

Ionic conductivity of the free-standing NaSIE electrolyte is measured in a symmetric stainless steel ss/NaSIE/ss cell. The NaSIE polymer electrolyte exhibits a promising ionic conductivity of 2×10^{-3} S cm^{-1} at 30 °C (Fig. 3a). The electrochemical stability of the solid-state electrolyte determines the voltages of the compatible electrodes, and the amount of potential parasitic reactions at both the anode and cathode sides. The electrochemical stability of the NaSIE polymer electrolyte is investigated via a CV test in a range between −0.5 V to 5 V at a scan rate of 0.5 mV s^{-1}. A typical sodium stripping and plating peak is observed at −0.5 V and 0.4 V. No obvious oxidation peaks up to 5 V were observed, revealing the extensive anodic stability.

The sodium transference number is also regarded as a critical property for polymer electrolyte as it is closely related to the
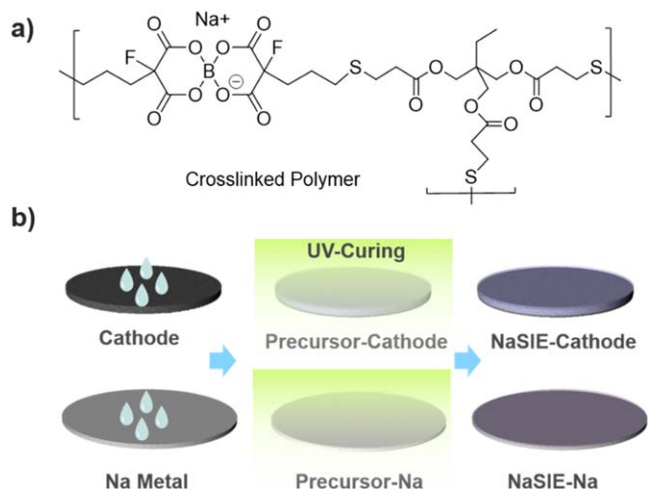
Figure 2. (a) Chemical structure of the NaSIE polymer electrolyte. (b) Schematic illustration of the NaSIE coating on sodium metal and NNMO electrodes.

propensity of sodium dendrite and dead sodium formation.[16] The sodium transference number of the NaSIE polymer electrolyte is measured via the Bruce-Vincent method:[12] a small overpotential (10 mV) is applied on to the symmetric Na/NaSIE/Na cell and the initial and steady current and the impedance changes are recorded. A steady current is observed during the constant potential hold (Fig. 4a). The sodium transference number (t_{Na}^{+}) is determined to be 0.91. This can be attributed to the immobilizing of the anions into the polymer network, enabling the sodium ion as the main movable species.

Overall, the stability of such a NaSIE towards the sodium metal can be investigated through sodium plating/stripping. The electrolyte with a high sodium transfer number is believed to suppress the concentration gradient and enable the stable sodium deposition. A symmetric Na/NaSIE/Na cell is used to plate and strip sodium at various current densities. As shown in Fig. 5a, the overpotential of 0.11 V, 0.21 V, 0.28 V, 0.39 V, 0.45 V, and 0.5 V is obtained at a current density of 0.02 mA cm^{-2}, 0.06 mA cm^{-2}, 0.1 mA cm^{-2}, 0.2 mA cm^{-2}, 0.3 mA cm^{-2}, and 0.4 mA cm^{-2}, respectively. When the current density is set back to 0.1 mA cm^{-2}, the overpotential recovers to 0.22 V. The long cycling of the stripping/plating test was applied at 0.1 mA cm^{-2} with five-minute intervals. After 10,000-min. cycling, stable voltage profiles are observed without obvious voltage vibrations.

The final step is the test of as-prepared NaSIE electrolyte in a coin cell using a configuration of Na//NNMO. The electrolyte is used in a flooded condition (120 μl), as currently we are not focusing on the optimization of cell format for achievement of an optimal high specific capacity or targeting its application for large format cell. Instead, we compare the SIE and conventional liquid sodium electrolyte, i.,,e, 1.0 M NaPF$_6$ in mixture of propylene carbonate and sulfolane (PC/SF). The cathode, NNMO (P2-Na$_{0.67}$Ni$_{0.33}$Mn$_{0.67}$O$_2$, while P denotes the prismatic crystal structure), is prepared by a solid-state reaction using co-precipitated precursor Ni$_{0.33}$Mn$_{0.67}$(OH)$_2$ with Na$_2$CO$_3$ salt followed by calcination, as previously reported by Dahn et al.[10]

The rate capability of the Na/NaSIE/NNMO cells equipped with NaSIE electrolyte is evaluated at rates from 0.1C to 2C. The cell delivers a reversible capacity of 85.7 mAh g^{-1}, 83.5 mAh g^{-1}, 80.5 mAh g^{-1}, 78.6 mAh g^{-1}, 74.0 mAh g^{-1}, 67.5 mAh g^{-1} and 56.9 mAh g^{-1} at 0.1C, 0.4C, 0.8C, 1C, 1.2C, 1.5C, and 2 C, respectively (Fig. 6a). When the current density is set back to 0.8C, a reversible capacity of 79.5 mAh g^{-1} is recovered. This demonstrates excellent sodium ion transportation inside the NaSIE polymer electrolyte. For the long cycling test, the cell exhibits a capacity retention of 86.7%, which was achieved after 150 cycles (Fig. 6b). The charge and discharge profiles of the cell equipped with NaSIE polymer electrolyte rate and cycling tests are presented in Figs 6c and 6d. Control cells run in triplicate using NaPF6 in the same solvents were also assembled and reported for comparison in Fig. S1 (Supplemental Information (available online at stacks.iop.org/JES/168/120543/mmedia)).

Discussion

Rational structural design.—As we discussed earlier, many of the inherent properties of the NaSIE originate from its molecular structures, with the emphasis on both the anion borate and the two pendant allyl groups to provide the α, ω-diene unit for UV-initiated crosslinking plasticizers in the polymer electrolyte. The other important key to the success of constructure of the interface friendly solid gel electrolyte is the that thiol−ene free-radical polymerization is adopted as an efficient, defect-free, and high-yield polymerization method. Mechanical properties are improved using multifunctional thiol end molecules together with α, ω-dienes. In our studies, trimethylolpropane tris(3-mercapto propionate) (TMPT) with three active thiol ends is selected as the thiol unit and for the UV-initiated polymerization. 2, 2-Dimethoxy-2-phenylacetophenone (DMPA) is used as the photo initiator. The electrochemical properties are improved, compared to the BOB (bis(oxalato) borate) family, through the introduction of a fluorinated structure. Electron
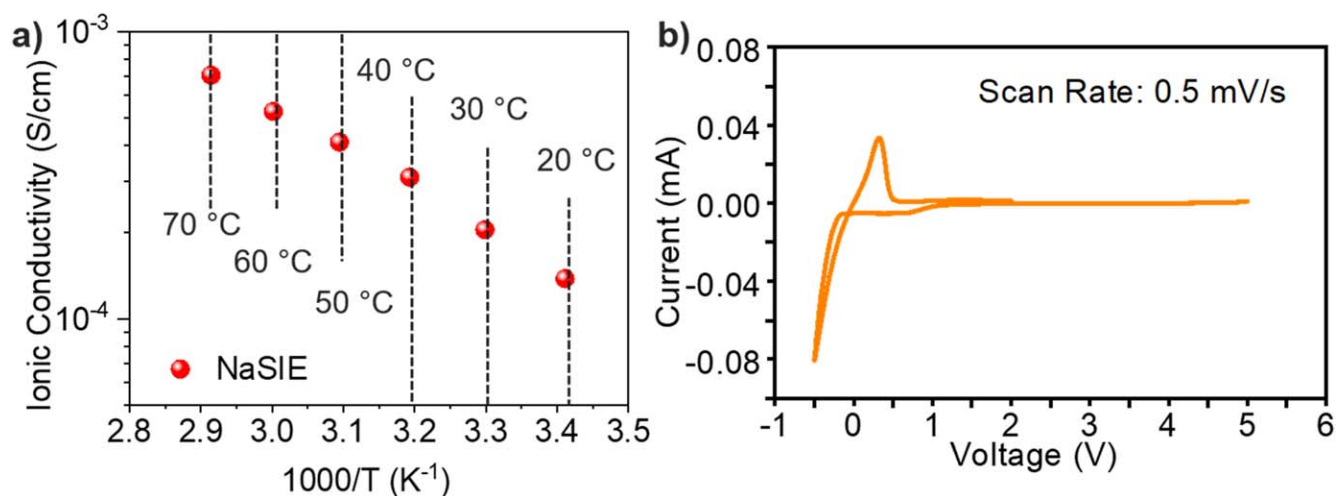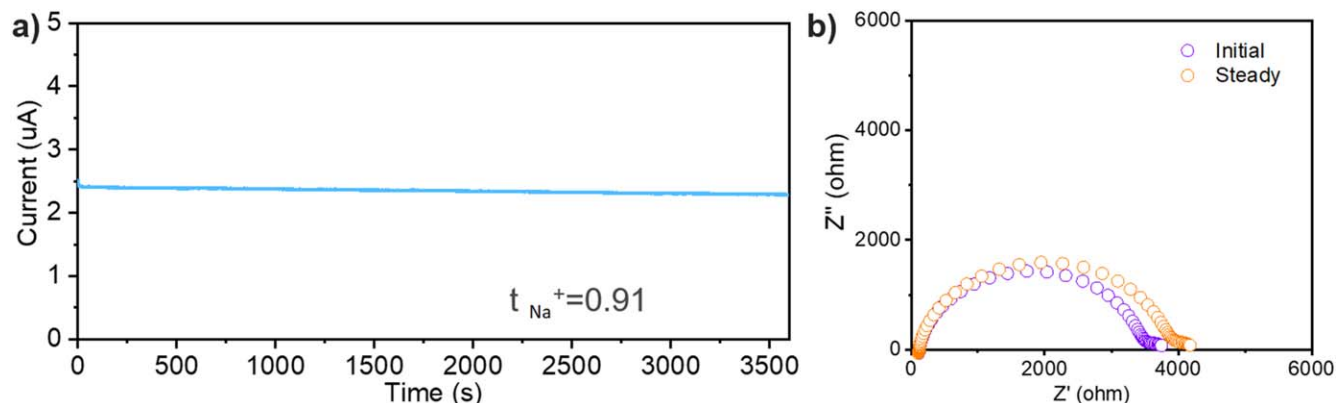

Figure 3. Electrochemical properties of the NaSIE electrolyte. (a) Ionic conductivities of NaSIE electrolyte at varying temperatures from 20 °C to 70 °C. (b) Cyclic voltammogram of a Na/NaSIE/SS asymmetric cell in a chemical window from −0.5 V to 5 V at a scan rate of 0.5 mV s^{-1}.

Figure 4. Transference number measurement of NaSIE electrolyte. (a) Chronoamperogram test of a Na/NaSIE/Na symmetric cell with an applied voltage of 10 mV. (b) Initial and steady-state internal resistance of Na/NaSIE/Na symmetric cell before/after polarization.
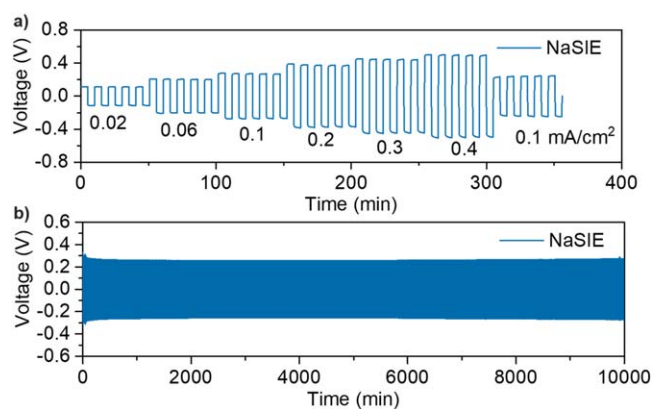

Figure 5. (a) Voltage profiles of stripping and plating in the symmetric cell at various current densities. (b) Galvanostatic cycling performance of the Na/NaSIE/Na symmetric cell at 0.1 mA cm^{-2}.

withdrawing groups such as F is known to increase the anodic stability of the sodium salt monomer owing to the strong electron-withdrawing nature of fluorine. As an adapted new solvent system to accommodate the change of the solubility, we improvise to use a mixture of sulfolane (SF)/propylene carbonate (PC) dissolve the salt. The high transference number (0.91) obtained for the NaSIE suggests a high critical current density; indeed, a CCD of 0.4 mA cm^{-2} is obtained for our NaSIE. The high CCD signals an easy metric for comparison of the performance. In fact, an eight-fold improvement in CCD is achieved through the structural design and change of chemicals, compared with a similar single-ion conducting electrolyte consisting of Na-poly(tartaric acid)borate (CCD = 0.05 mA cm^{-2}).[7]

Interfacial stability.—The interfacial stability is also investigated using post-mortem characterizations as impedance rise, dendrite formation, as well as decomposition product can all be correlated with interface. For example, after the cycling of the cells, the images of the electrolytes and electrodes are subjected to further analysis.
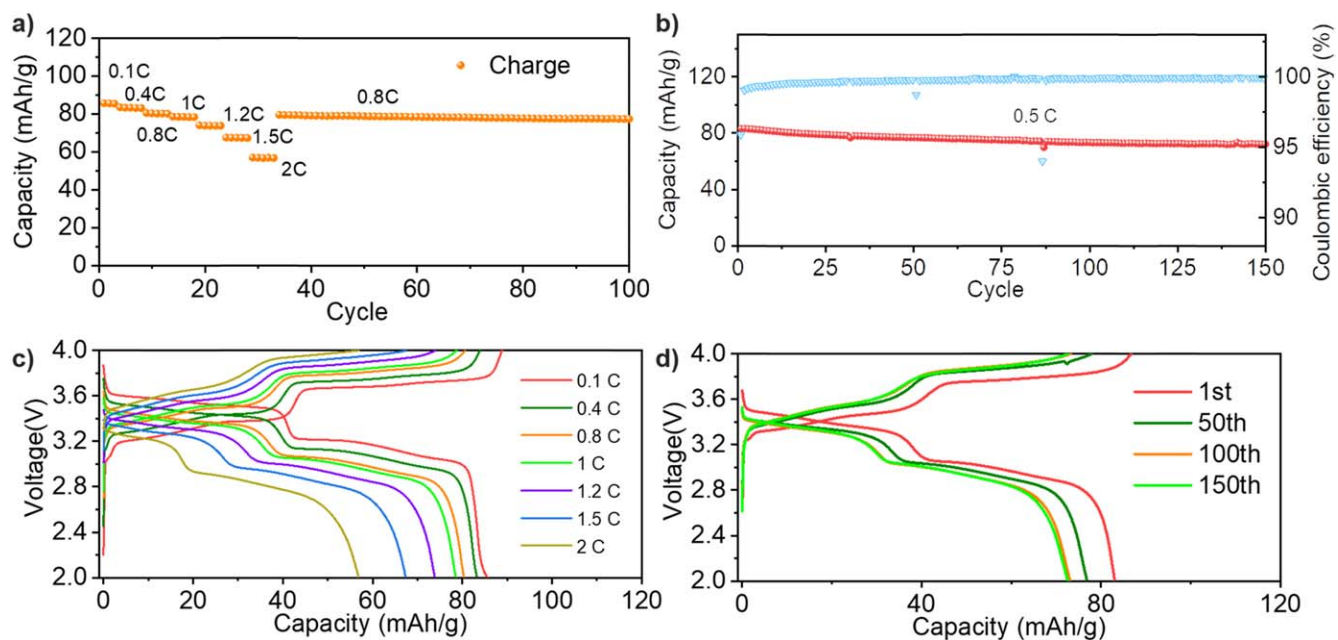

Figure 6. Battery performance for Na/NaSIE/NNMO cells. (A) Rate capability tests of Na/NaSIE/NNMO cells at various current densities. (B) Cycling performance of the Na/NaSIE/NNMO cell at 0.5C. c) Galvanostatic charge and discharge profiles of Na/NaSIE/NNMO cells at various current densities. (D) Galvanostatic charge and discharge profiles of Na/NaSIE/NNMO long-cycle cells at indicated cycles.

As shown in Figs. 7a–7b and S2, the NaSIE not only retains the high specific capacity, but also prevents the deterioration or reaction of active sodium metal with the electrolyte. The electrolytes are also collected by dissolving the separator and electrodes in $CDCl_3$ after aging; the NMR spectrum is shown in Fig. 7b. Presence of decomposition products (mark with an asterisk) are also found with the cycled $NaPF_6$ electrolyte. On the contrary, there is no visible change on the surface of the cycled NaSIE. (Fig. S2).

The SEM images of the cathode//SIE//Na shows a seamless incorporation of the SIE, covering all the pores and roughness of the cathodes, suggesting that the softness of the polymer is capable to create a nice and uniform surface. To ensure good contact between the electrolyte and electrode surface, a premixed solution containing NaBFMB and plasticizer was drop-cast onto the sodium metal and cathode laminate separately, as shown in Fig. 8. This procedure allows the fluid-like precursor to accommodate the porosity and rough surface of the composite cathode disk through the wetting and infiltration process. After 15 min of static standing, the electrolyte is cured on top of the sodium metal and cathode through 15 min of UV–visible light (vis) exposure. The EDAX (Energy-dispersive X-ray spectroscopy) element mapping of elements S and F, that are unique and sourced only from the polymer, are well dispersed within both the polymer electrolyte and the cathodes. Figure 8a demonstrates the homogeneity of the SIE with distribution of F and S equally throughout the electrolyte. As shown in Fig. 8 b3–4 and b6–7, the observation that S and F appear in the same area as Ni and Mn demonstrates the infiltration of the liquid into the porous cathode. Note that after curing, they can be pressed together through the polymer side to construct a Na/NNMO battery.

After the cycling, the stability of the anode is examined through X-ray photoelectron spectroscopy (XPS). XPS characterization is the best technique to study the SEI formation on sodium metal electrode. It is a surface technique that allows specific detection of elemental species within the depth of 10 nm. Because its sensitivity and element-specific property (it can identify the species and the bonding environment through the kinetic energy), it is widely used for studies of the stability of both the cathodes and anodes. XPS studies were carried out on the sodium metal electrodes of the Na/NaSIE/NNMO and Na/NaPF$_6$/ NNMO cells after 100 cycles. Assignments of peaks with binding energy are according to the NIST XPS database and previous works.[17–20] In the C 1s and O 1s spectra (Figs. 9d, 9e), higher carbonyl containing groups (–O–C(=O) –O, –O–C=O, C=O) content were observed with respect to C–H/C–C on the sodium metal electrode cycled in the liquid electrolyte of $NaPF_6$/PC/SF than that cycled with NaSIE, indicating the further decomposition of the organic solvents in $NaPF_6$, which agrees with the NMR data. In the F 1s spectra (Fig. 9c), the peak located at 685.3 eV is assigned to the F–Na bond from NaF. As shown in Figs. S3–4, after the same sputtering time to remove the SEI layer on the Na anode, the intensity for C1s in Na SIE is higher than that of in liquid electrolyte (LE). The Na signal is much stronger in LE also indicates the SEI layer from LE is thinner. Atomic concentration data also suggests that organic SEI components are higher for SIE than LE (Tables S1–2). This agrees with our previous observation of organic fluorine component enabling SEI and improving columbic efficiency.[14]

As shown in Table S3, model calculations are performed to simulate the ion concentration change under an applied current density (0.1 mA cm^{-2}) in a symmetric Na/NaSIE/Na and the non-crosslinked Na/NaPF$_6$ (PEO)/Na with respect to time. The cell parameters such as thickness and operating temperature are defined in Table S4. An initial salt concentration is set as 1000 mol m^{-3} for both electrolytes, and due to their intrinsic different ionic conductivity and transference number, different Fickian diffusion coefficients of 8.87e^{-12} m^2 s^{-1} for the NaSIE electrolyte and 8.31e^{-12} m^2 s^{-1} for the non-cross-linked electrolyte are obtained. The ion concentration changes with respect to time in the first five minutes are shown in Fig. 10, with NaSIE showing a minimum ion concentration gradient increase, while non-crosslinked sodium electrolyte clearly showing cation and anion gradient concentration increases at different ends of the polarization. Note that the CCD of NaSIE, despite the high
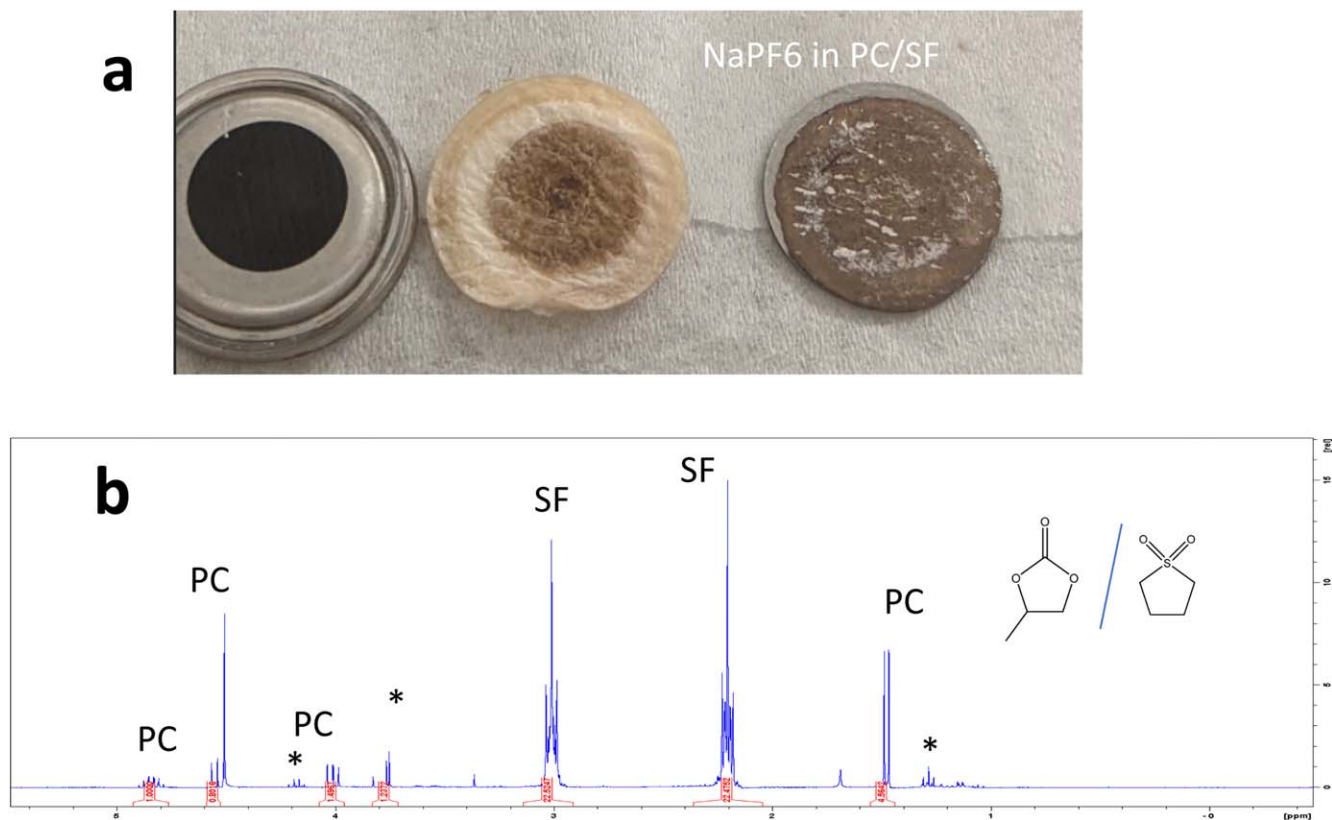

Figure 7. The image of dissembled Na//NNMO cells using 1.0 M $NaPF_6$ in PC/SF solution. The NMR shows both characteristic peaks that belong to PC/SF, as well as unidentified peaks.
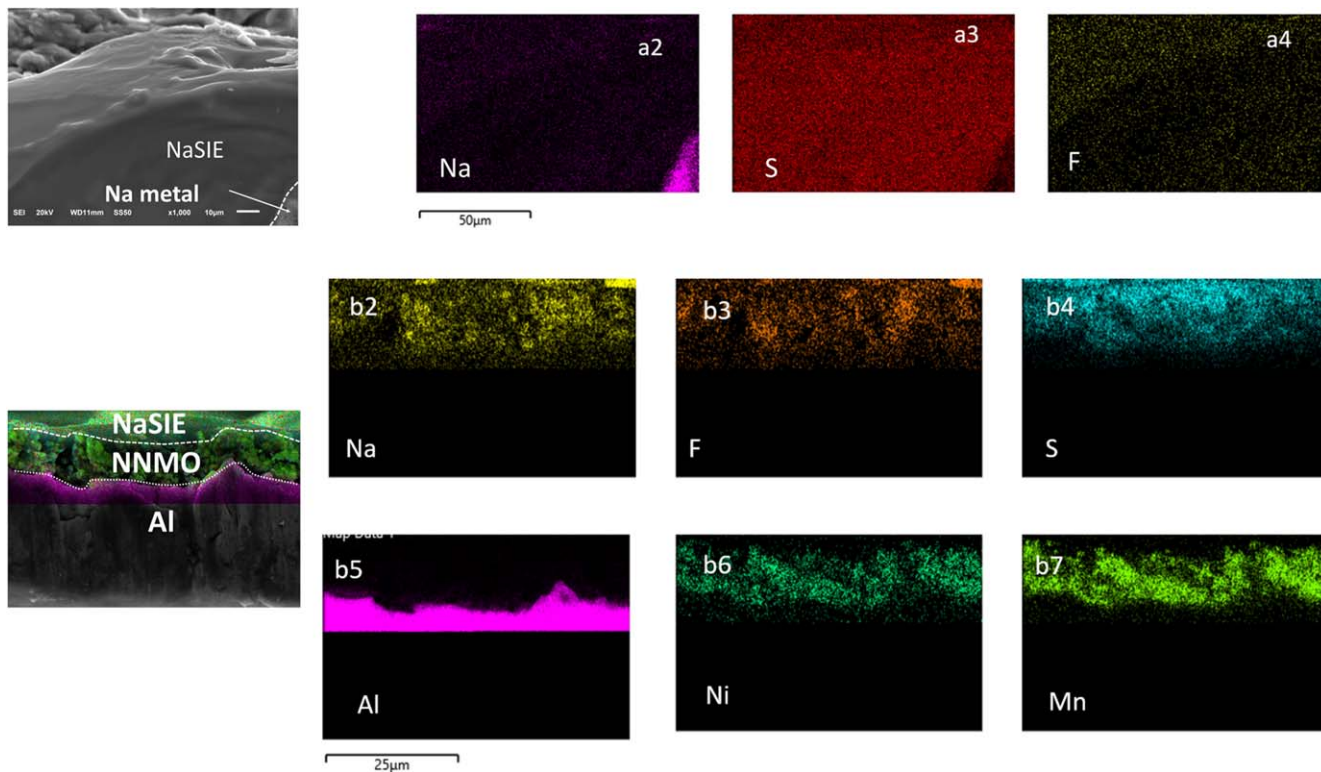
Figure 8. Morphological characterization of the in situ coated NaSIE electrodes. The polymer precursors were drop-cast onto the electrode surface and left for 20 min, followed by photocrosslinking. t. (a) Scanning electron microscope (SEM) and EDAX characterization of cross- sections NaSIE on sodium metal electrode (a1)–(a5) and NNMO cathode (b1)–(b7), respectively.
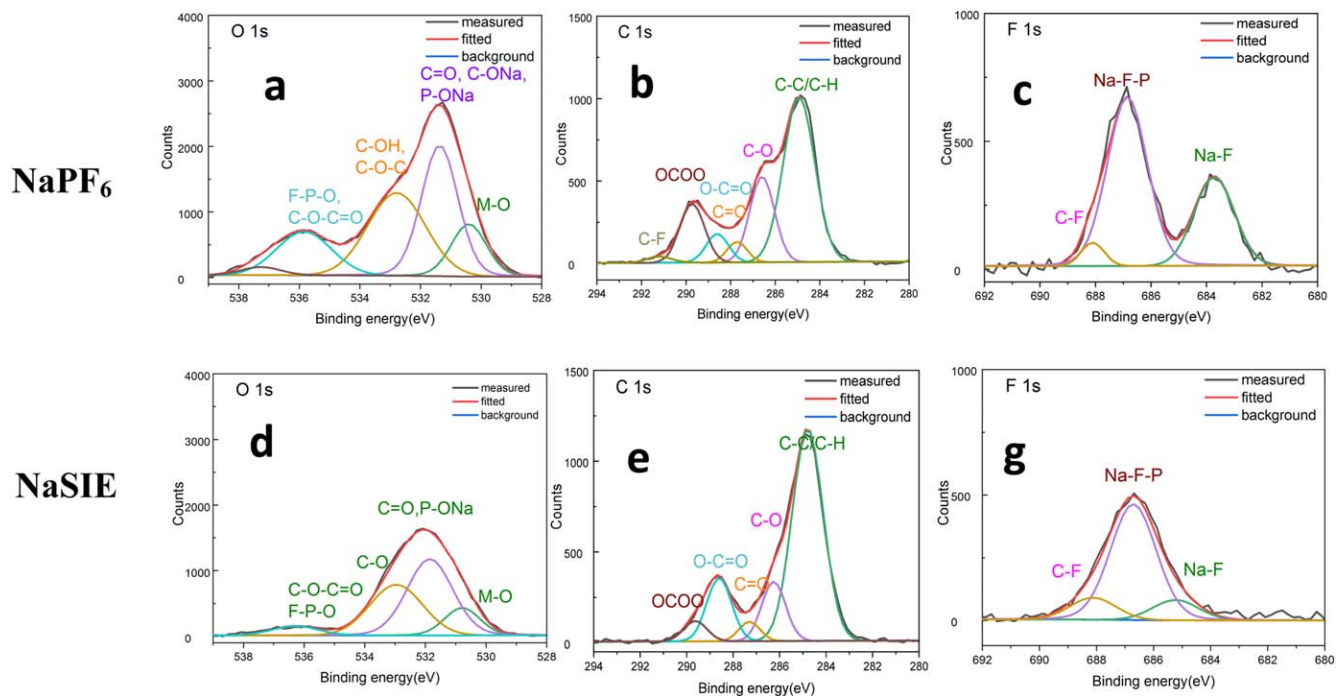

Figure 9. XPS characterizations of cycled sodium metal electrodes. (a–c) O 1s, C 1s, and F 1s spectra of the cycled sodium metal electrode in the Na/NaPF$_6$/NNMO cell. (d–f) O 1s, C 1s, and F 1s spectra of the cycled sodium metal electrode in the Na/NaSIE/NNMO cell. For the O 1s spectra, the peak at 534.9 eV corresponds to oxygen atoms that are bound to groups as in C–O–C=O, F–P–O. The orange peak at 532.9 eV is attributed to C–OH and C–O–C bonds. The peak at 531.9 eV corresponds to the several C–ONa, P–Ona moieties and oxygen atoms that are doubly bound to carbon or phosphorus atoms as C=O or P=O. The Metal–O bond has a binding energy of 530.7 eV. The C 1s spectra are deconvoluted into a light green peak corresponding to hydrocarbon (C–H/C–C, 284.8 eV), a purple peak corresponding to ether carbon (C–O–C, 286.3 eV), a beige peak corresponding to a carbonyl group (C=O, 287.3 eV), and a blue peak corresponding to the (–O–C=O) bond at 288.5 eV, and a brown peak corresponding to carbonyl group in ((–O–C(=O) –O) at 289.8 eV, and an olive color peak at 291.3 eV corresponding to C–F bond (only present in the NaSIE case). For the F 1s spectra, the green peak corresponds to NaF (F–Na, 687.3 eV), and the beige peak is assigned to organic fluorine(F–C, 687 eV).
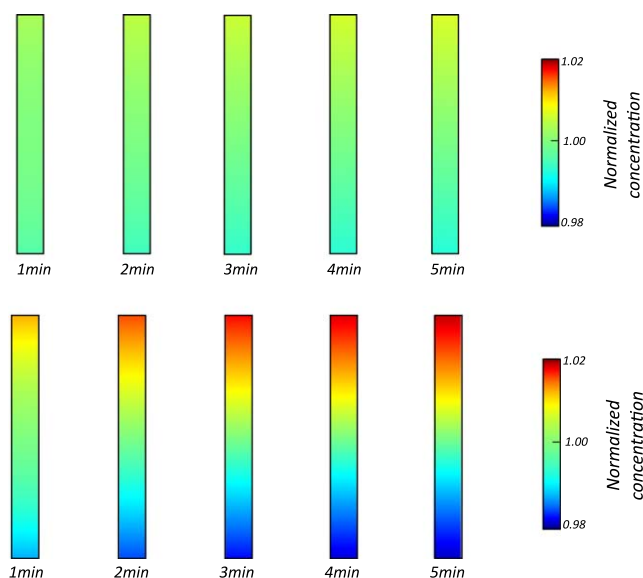
Figure 10. Na^+ concentration distribution profiles of NaSIE (top) and the non-cross-linked PEO electrolyte (bottom) in sodium symmetric cells at 0.1 mA cm^{-2}. The finite element method is applied and conducted via COMSOL.

conductivity, is still inferior to that of the $NaPF_6$ liquid electrolyte.[21] The diffusivity (8.87×10^{-12} m^2 s^{-1}), for example, is more than one order of magnetitude lower than that of the liquid analog (1.34×10^{-10} m^2 s^{-1}). The transport properties of the electrolyte is especially important for applications such as Li/Na metal batteries or extreme fast charging. Several factors consist that of the transport properties, including conductivity, salt diffusivity, transference number, electrolyte density, and thermodynamic factor.[22] A high CCD, essentially reflecting all the parts of transport properties, needs more than a relatively high ionic conductivity and transference.

Conclusions

In this work, we have designed and synthesized a single-ion conducting polymer electrolyte for sodium ion batteries. Unlike the previous report, this SIE electrolyte has strength in both electrochemical and interfacial stability. The key to successful preparation of the SIC electrolyte includes the synthesis of the NaBFMB and the thiol-ene reaction. The NaSIE polymer electrolyte exhibits a promising ionic conductivity of 2×10^{-3} S cm^{-1} at 30 °C, owing to the sp^3 boron center with low dissociation energy. By virtue the anions are anchored into the polymer network, a high Na ion transference number of 0.91 is achieved. A stable sodium deposition is observed in the stripping and plating test at 0.1 mA cm^{-2} for 10,000 min test. The NNMO based Na-ion batteries equipped with the NaSIE polymer electrolyte demonstrates a stable cycling performance for 150 cycles with a capacity retention of 86.79%. The superior cycling performance confirms our hypothesis of the positive effects from both the high electrolyte anodic stability and low interfacial resistance.

Acknowledgments

ORCID

Chen Liao https://orcid.org/0000-0001-5168-6493

References

1. S. Liu, S. Tang, X. Zhang, A. Wang, Q.-H. Yang, and J. Luo, "Porous al current collector for dendrite-free na metal anodes." *Nano Lett.*, **17**, 5862 (2017).
2. J. Gao, C. Wang, D.-W. Han, and D.-M. Shin, "Single-ion conducting polymer electrolytes as a key jigsaw piece for next-generation battery applications." *Chem. Sci.*, **12**, 13248 (2021).
3. J. Zhu, Z. Zhang, S. Zhao, A. S. Westover, I. Belharouak, and P.-F. Cao, "Single-ion conducting polymer electrolytes for solid-state lithium–metal batteries: design, performance, and challenges." *Adv. Energy Mater.*, **11**, 2003836 (2021).
4. Z.-Y. Gu, J.-Z. Guo, X.-X. Zhao, X.-T. Wang, D. Xie, Z.-H. Sun, C.-D. Zhao, H.-J. Liang, W.-H. Li, and X.-L. Wu, "High-ionicity fluorophosphate lattice via aliovalent substitution as advanced cathode materials in sodium-ion batteries." *InfoMat*, **3**, 694 (2021).
5. H.-J. Liang, Z.-Y. Gu, X.-X. Zhao, J.-Z. Guo, J.-L. Yang, W.-H. Li, B. Li, Z.-M. Liu, W.-L. Li, and X.-L. Wu, "Ether-based electrolyte chemistry towards high-voltage and long-life na-ion full batteries." *Chemie International Edition*, **60**, 26837 (2021).
6. G. Yan, S. Mariyappan, G. Rousse, Q. Jacquet, M. Deschamps, R. David, B. Mirvaux, J. W. Freeland, and J.-M. Tarascon, "Higher energy and safer sodium ion batteries via an electrochemically made disordered Na3V2(PO4)2F3 material." *Nat. Commun.*, **10**, 585 (2019).
7. L. Yang, Y. Jiang, X. Liang, Y. Lei, T. Yuan, H. Lu, Z. Liu, Y. Cao, and J. Feng, "Novel Sodium–poly(tartaric acid)borate-based single-ion conducting polymer electrolyte for sodium–metal batteries." *ACS Appl. Energy Mater.*, **3**, 10053 (2020).
8. P. G. Bruce and C. A. Vincent, "Steady state current flow in solid binary electrolyte cells." *J. Electroanal. Chem. Interfacial Electrochem.*, **225**, 1 (1987).
9. C. Liao et al., "Synthesis and characterization of lithium bis(fluoromalonato)borate for lithium-ion battery applications." *Adv. Energy Mater.*, **4**, 1301368 (2014).
10. F. Zhou, X. Zhao, A. van Bommel, A. W. Rowe, and J. R. Dahn, "Coprecipitation Synthesis of Ni$_x$Mn$_{1-x}$(OH)$_2$ Mixed Hydroxides." *Chem. Mater.*, **22**, 1015 (2010).
11. Y. Xie et al., "Role of lithium doping in P2-Na$_{0.67}$Ni$_{0.33}$Mn$_{0.67}$O$_2$ for sodium-ion batteries." *Chem. Mater.*, **33**, 4445 (2021).
12. P. G. Bruce, J. Evans, and C. A. Vincent, "Conductivity and transference number measurements on polymer electrolytes." *Solid State Ionics*, **28-30**, 918 (1988).
13. Z. Yang, J. W. Morrissette, Q. Meisner, S.-B. Son, S. E. Trask, Y. Tsai, S. Lopykinski, S. Naik, and I. Bloom, "Extreme Fast-Charging of Lithium-Ion Cells: Effect on Anode and Electrolyte." *Energy Technology*, **9**, 2000696 (2021).
14. K. Liu et al., "Molecular design of a highly stable single-ion conducting polymer gel electrolyte." *ACS Appl. Mater. Interfaces*, **12**, 29162 (2020).
15. E. J. Cheng, A. Sharafi, and J. Sakamoto, "Intergranular Li metal propagation through polycrystalline Li$_{6.25}$Al$_{0.25}$La$_3$Zr$_2$O$_{12}$ ceramic electrolyte." *Electrochimica Acta 2017*, **223**, 85.
16. W. Ling, N. Fu, J. Yue, X.-X. Zeng, Q. Ma, Q. Deng, Y. Xiao, L.-J. Wan, Y.-G. Guo, and X.-W. Wu, "A flexible solid electrolyte with multilayer structure for sodium metal batteries." *Adv. Energy Mater.*, **10**, 1903966 (2020).
17. X. Ren et al., "Role of inner solvation sheath within salt–solvent complexes in tailoring electrode/electrolyte interphases for lithium metal batteries." *Proc. Natl Acad. Sci.*, **117**, 28603 (2020).
18. Y. Lu, Y. Cai, Q. Zhang, L. Liu, Z. Niu, and J. Chen, "A compatible anode/succinonitrile-based electrolyte interface in all-solid-state Na–CO$_2$ batteries." *Chem. Sci.*, **10**, 4306 (2019).
19. J. Fondard, E. Irisarri, C. Courrèges, M. R. Palacin, A. Ponrouch, and R. Dedryvère, "SEI composition on hard carbon in Na-ion batteries after long cycling: influence of salts (NaPF6, NaTFSI) and additives (FEC, DMCF)." *J. Electrochem. Soc.*, **167**, 070526 (2020).
20. B. Han, Y. Zou, Z. Zhang, X. Yang, X. Shi, H. Meng, H. Wang, K. Xu, Y. Deng, and M. Gu, "Probing the Na metal solid electrolyte interphase via cryo-transmission electron microscopy." *Nat. Commun.*, **12**, 3066 (2021).
21. D. Morales, R. E. Ruther, J. Nanda, and S. Greenbaum, "Ion transport and association study of glyme-based electrolytes with lithium and sodium salts." *Electrochim. Acta*, **304**, 239 (2019).
22. A. Mistry and V. Srinivasan, "Do we need an accurate understanding of transport in electrolytes?" *Joule*, **5**, 2773 (2021).